

GODDARD  
GRANT

IN-43-CR

146427

298

Semi-Annual Status Report

Period: March 1987-March 1988

to

National Aeronautics and Space Administration

NASA Grant No. NAG 5-919

AN UPDATE ON REMOTE MEASUREMENT OF SOIL MOISTURE OVER VEGETATION  
USING INFRARED TEMPERATURE MEASUREMENTS:  
A FIVE PERSPECTIVE

Submitted by:

Toby N. Carlson

Department of Meteorology  
The Pennsylvania State University  
University Park, PA 16802

(NASA-CR-182926) AN UPDATE ON REMOTE  
MEASUREMENT OF SOIL MOISTURE OVER VEGETATION  
USING INFRARED TEMPERATURE MEASUREMENTS: A  
FIVE PERSPECTIVE Semiannual Status Report,  
Mar. 1987 - Mar. 1988 (Pennsylvania State

N88-24109

Unclas  
G3/43 0146427

June 1988

## ABSTRACT

We are undertaking a multifacet research effort consisting of model development, image analysis and micrometeorological measurements. The object of our research is to push beyond the present limitations of using the infrared temperature method for remotely determining surface energy fluxes and soil moisture over vegetation.

Model development consists of three aspects: (1) a more complex vegetation formulation which is more flexible and realistic, (2) a method for modeling the fluxes over patchy vegetation cover and (3) a method for inferring a two-layer soil vertical moisture gradient from analyses of horizontal variations in surface temperatures. . In the future, we will use HAPEX and FIFE satellite data along with aircraft thermal infrared and solar images, as input for the models. To test the models, moisture availability and bulk canopy resistances will be calculated from data collected locally at the Rock Springs experimental field site and, eventually, from the FIFE project.

## 1. Background

For over ten years we have been interested in remote measurement of soil moisture and surface energy fluxes using thermal infrared temperatures. We began this investigation because of the need for providing initial soil moisture values for atmospheric prediction models. Our technique is conceptually very simple: a one-dimensional, time-dependent boundary layer model is inverted in conjunction with measured radiometric surface temperatures, obtained by satellite, aircraft or surface-based radiometers. The model then simulates the surface fluxes, soil moisture availability and thermal inertia. We have applied this method rather successfully to regions ranging in size from a large city up to that of a state (Carlson et al., 1981; Carlson et al., 1984; Carlson, 1986; Flores and Carlson, 1987). The method demonstrates a high correlation between antecedent precipitation and the soil moisture parameter, which is the moisture availability. Similar results were obtained by Wetzal and his co-workers (e.g. Wetzal and Woodward, 1987).

By 1984, however, it became clear to us that in order to advance our method beyond its current level of scientific utility, a very great deal of additional thought and experimentation (both in terms of modeling and measurement) would be required to overcome some serious conceptual difficulties. The problems lie in the complex nature of the surface canopy, particularly vegetated surfaces, and the fundamental inadequacies of mechanistic models for representing plant behavior. Vegetated surfaces are difficult to model because parameters are subject to the needs of a living community of plants with differing architecture and phenological behavior. Moreover, the energy fluxes over plant canopies are modulated by the nature of the soil surface below and the density and fractional cover of the

vegetation. One realizes that the resolution of such complexity is elusive because the methods available are called upon to unscramble the information from just a few available measurements.

Beginning in 1984 we undertook to model vegetation. Cooperation with French scientists resulted in the publication of a paper concerning the development of a vegetation model (Taconet et al., 1986). Results of this paper and subsequent analyses led to some interesting conclusions. First, the vegetation parameterization improved estimates of surface energy fluxes (and, with less certainty, the soil moisture) for a wheat canopy in a controlled experiment involving a combination of ground micrometeorological measurements and satellite data. It was clear, however, that our ability to calculate reasonable values of evapotranspiration and surface sensible heat flux, given the accuracy of the initial conditions supplied to the model, is intimately dependent on the correct formulation of the stomatal resistance function and a knowledge of the amount of vegetation present. Second, due to inherent errors, changes in surface energy fluxes or soil moisture cannot be resolved except during a water limitation phase of drying. Perry and Carlson (1988) show that uncertainties in the model and in the ground measurements impose an inherent and irreducible error on the infrared technique. They suggest that a certain minimum surface temperature variance must be present in order to calculate meaningful values of surface energy fluxes. The situation is even more precarious over vegetation than bare soil, particularly when the object is to measure spatial variability of surface fluxes. Not only are plants complex in their architecture, but they are able to regulate the water loss and so maintain a high level of transpiration until water limitation is reached. Thus, the measured surface temperatures or surface fluxes hardly change with changing soil moisture if the plants are

not in a state of water limitation. Numerous experimental investigations (e.g. Turner, 1974; Turner, 1975; Thomas et al., 1975; Fisher et al., 1981; Stewart and Dwyer, 1983; Dwyer and Stewart, 1984) show that the stomatal resistance increases very rapidly (with associated collapse in transpiration) as the substrate water content begins to reach a water limitation threshold. The significance of this water limitation threshold for remote sensing is that variations in leaf temperature theoretically become detectable by satellite or aircraft radiometers at soil water content near or below the water limitation threshold.

Various models based on direct experimental evidence (e.g. Jarvis, 1976; Federer and Gee, 1976; Federer, 1979; Choudhury, 1983; Avissar et al., 1985) describe the exponential behavior of bulk stomatal resistance ( $r_{st}$ ) near a drying threshold and also the effect of other external parameters, such as sunlight, vapor pressure deficit and air temperature. (Sunlight also exhibits a threshold for stomatal resistance, but the effect is not important since it occurs at low values of insolation.) Unfortunately, the parametric form of the models differs widely from one model to the next and the coefficients in these models are poorly known or pertain to one specific species, climate and set of soil conditions. Present lack of knowledge of these parameters is understandable in view of (1) the mechanistic nature of models that attempt to describe the behavior of living entities in terms of simple formulae and (2) the sensitivity of the specified parameters to phenology, soil conditions and the past history of the plant.

## 2. Current research objectives

We view the present state of modeling surface energy fluxes and substrate water content over vegetated canopies as dependent on carrying it out the

following projects: (1) The specification of the stomatal and xylem resistance functions and the drying threshold for a few broad classes of vegetation, (2) the modeling of a mixed canopy in which substantial areas of bare soil and leaf surfaces are visible, (3) the determination of the biomass, leaf area index or percentage vegetation cover and (4) the gathering of micrometeorological measurements for model testing. These four items constitute integral components of our proposed work. Below, we address them in presenting an overview of research carried out during the previous year.

a) Modeling stomatal resistance

The basic framework of our boundary layer model is described in Carlson (1986) and Taconet et al. (1986). Recently, we have reformulated the plant model to include (1) a more realistic stomatal resistance function and (2) a more comprehensive and precise link between stomatal resistance, plant-soil potential differences and substrate moisture. This model architecture is outlined in Fig. 1. The main point of departure with our earlier vegetation model is the inclusion of a xylem (stem plus root) resistance and a flow of moisture from soil to root. Two equations are necessary to describe the flow of water from the soil to the atmosphere through the plants. One is the leaf transpiration equation

$$L_e E_f = \frac{\rho L_e (q_{\ell}(T_{\ell}) - q_{af})}{r_{st} + r_{af}} \quad (1)$$

and the other is the xylem water flow equation

$$F_W = \frac{\psi_g - \psi_l - \rho_w g h}{Z_p + Z_g} \quad (2)$$

where  $L_e E_f$  is the transpiration,  $r_{st}$  is the stomatal resistance,  $e_\ell(T_\ell)$  the saturation vapor pressure at the temperature of the leaf ( $T_\ell$ ),  $q_{af}$  the interplant air space specific humidity,  $r_{af}$  the resistance to water vapor flow from the leaf to interplant airspaces,  $Z_p$  the resistance to liquid water flow through the stem and roots (the sum of  $Z_{stem}$  and  $Z_{root}$ ),  $\psi_1$  the leaf water potential,  $\psi_g$  the ground water potential,  $Z_g$  the resistance to water flow from soil to root,  $r_g$  the resistance to the flow of water from soil to air and  $L_e E_g$  the soil evaporation; the symbol  $\theta$  (with various subscripts) refers to the volumetric liquid water content in the subsoil at various substrate levels. (Other symbols are not relevant to this immediate discussion.) In (2) the flow of water from soil to leaf is prescribed in terms of the appropriate resistances, the leaf-ground water potential difference corrected for the gravitational decrease of the leaf-ground potential drop (which is a function of the leaf height above soil ( $h$ ) and the density of water  $\rho_w$ ).

The bulk stomatal resistance ( $r_{st}$ ) and the average leaf resistance to water vapor flux ( $r_s$ ) are given by the following expressions:

$$r_s = aV (f\psi_\ell) f(S) \quad (3)$$

$$r_{st} = r_s / LAI$$

where  $A$  is a constant,  $V$  is the vapor pressure deficit in the atmosphere,  $LAI$  is the leaf area index and the functions  $f(\psi_\ell)$  and  $f(S)$  describe the effect of leaf water potential and solar radiation on  $r_{st}$ . Equations (1) and (2) resemble those used by Sellers (1985), Wetzell and Chang (1987), Federer and Gee (1976), Federer (1979) and Jarvis (1976).

Our formulation, though superficially similar to versions in the literature, differs somewhat in that we equate (1) and (2) and, given the soil moisture content and the function (3), we calculate  $L_e E_f$ ,  $\psi_\ell$  and  $\psi_g$ . Fig. 2 illustrates the exponentiality of the  $f(\psi_\ell)$  function and its effect on limiting the transpiration. Neglecting gravitational effects, transpiration is proportional to the difference between the ground and leaf potentials ( $\psi_g$  and  $\psi_\ell$ ). The function  $f(\psi_\ell)$  increases very rapidly with decreasing  $\psi_\ell$  at the right-hand side of the curve. The function form of  $f(\psi_\ell)$  is related to the ground water content ( $\theta$ ) via a characteristic relationship between  $\theta$  and  $\psi_g$ . By linking  $\theta$  with  $\psi_g$  and  $\psi_\ell$ , we have a consistent method for relating substrate water content to radiometric surface temperature and moisture availability.

Our version of (3) is somewhat similar to that of Avissar et al., (1985) except that it is expressed in terms of linear functions, rather than exponentials. For vapor pressure deficit the function increases in proportion to  $V$ . For  $f(\psi_\ell)$  and  $f(S)$ , the linear function captures the threshold effect by specifying the functions as straight lines but with very different slopes on either side of the threshold; the linear model is represented by the thin dashed lines in Fig. 2. This simplification allows us the flexibility to more easily fit the function (equation (3)) to vastly differing types of field data, while capturing the essentials of the exponentiality. Moreover, this version allows us to solve analytically for  $\psi_\ell$  and the transpiration.

Although the canopy structure represented in Fig. 1 and its governing equations appears to be unresolvable within the context of remote sensing applications, (because of a proliferation of additional constants that are unknowable), the solution for  $\psi_\ell$ ,  $\psi_g$  and for  $L_e E_f$  are critically dependent on

only one parameter, which is the leaf potential threshold, denoted as  $\psi_c$  in Fig. 2. As stated above, this threshold governs the rise of leaf temperature with decreasing substrate water content. Some experimental evidence is available for choosing realistic values of the critical  $\psi_c$  by species (Korner et al., 1979).

Our present objectives with regard to the vegetation parameterization have been to (1) finish sensitivity tests of the formulation based on the above equations, (2) test the model with local (single point) experimental measurements, (3) determine realistic values of the parameters that are appropriate for 3 or 4 major classes of vegetation under differing atmospheric conditions and (4) use the model in larger-scale applications.

b) Workshop on stomatal resistance

A proposed workshop on stomatal resistance has occupied much of our time. This workshop will be sponsored jointly by Penn State (using funds from this grant) and by the Remote Sensing Laboratory, Agricultural Research Service, Beltsville, Maryland. The goals of the workshop are necessarily very narrow: (1) to foster cooperation between modelers and experimenters involved in the use or development of stomatal resistance functions for larger-scale and remote sensing applications and (2) develop a more systematic methodology for the parameterization of stomatal and plant resistance in boundary layer models. An important objective is to maintain an intimate atmosphere at the workshop in order to encourage exchange of ideas. For that reason, the size of the workshop will be limited to not much more than 35 participants. A projected end product of the workshop will be a dedicated volume in Agriculture and Forest Meteorology devoted to summarizing the state of the art in modeling stomatal and plant resistance. We view this workshop as a major contribution to this subject.

The invitees comprise some of the most distinguished scientists in the field of modeling and measurement of stomatal and plant resistances. A significant fraction of our time has already been spent in planning the workshop. We are currently seeking additional funds from the NSF to cover participant travel.

c) Modeling the mixed canopy

Due to the differences in the rate of drying of a shallow bare soil surface versus a deep root-zone layer, radiometric surface temperatures may differ markedly between bare soil and vegetation even if vertical profiles of soil moisture are identical. We can illustrate this idea in the radiometric measurements made during the French HAPEX experiment. Fig. 3 shows the radiometric surface temperatures over an area comprising bare plowed fields (field N1), a young corn crop (field N6) and a full oats crop (field N2). Differences in temperature between bare soil ( $55-58^{\circ}\text{C}$ ), partial cover ( $47.7^{\circ}\text{C}$ ) and the oats ( $30.7^{\circ}\text{C}$ ) is very striking. Stomatal resistance measurements made in field N6 show that the young corn crop was not experiencing water limitation in the root zone (Fig. 4); moreover, there was virtually no temporal variation in the minimum daily value of  $r_{st}$  with changing water content in the root zone; an indication that the plants were not experiencing water stress.

On the other hand, the bare soil surface became desiccated after only about two weeks without significant rainfall or irrigation. Gravimetric sampling shows that the water content very near the surface was almost zero in various fields. Below the top 5 cm, however, the soil was relatively wet and certainly well above any water limitation threshold (the wilting point), which was probably near 10%. The composite vertical profile of soil moisture for the 16th of June is shown in Fig. 4.

It is clear, therefore, that horizontal variations in radiometric surface temperature are highly modulated by the amount of vegetation present (more precisely, the percent of unshaded bare soil cover visible to the radiometer). The boundary layer model, no matter how clever the vegetation formulation, must take account of this effect. Unfortunately, as stated by Lindroth and Halldin (1986), one-dimensional vegetation parameterizations are likely to fail as the leaf area index decreases to values of about 1.0.

### Methodology

Rather than treat surface inhomogeneity as a cause for despair, we are endeavoring to extract information concerning the vertical profile of soil moisture from horizontal variations in surface temperature. This idea of deriving a two-level vertical profile of soil moisture from horizontal variations of surface temperature is new and has not been fully tested. (We should point out that the problem of inhomogeneous surface temperatures is not the same as discussed by Wetzell and Chang (1987).) Let us imagine a sample of pixel measurements made in the thermal infrared and at various solar wavelengths over a surface such as that shown in Fig. 3. Surface temperatures are calculated from the thermal infrared radiances and leaf area index values from the solar radiances (the technique of converting visible radiances to leaf area index is discussed below). Preliminary inspection of the HAPEX data suggests a distribution of surface temperature ( $T_s$ ) versus leaf area index (LAI) such as that shown in Fig. 5.

A first step in the solution of this problem was to relate visible channel radiance, specifically the normalized difference vegetation index (NDVI), to the leaf area index (LAI), which serves as a measure of the amount of vegetation in our boundary layer model. We perform this comparisons over

relatively homogeneous surface areas such as that shown in Fig. 3. We are currently exploring the use of various formulae relating NDVI to LAI, including that of Bauer et al. (1985), and comparing them with our own function derived from aircraft and ground-based measurements made during HAPEX.

The next step is to derive the functional relationship between LAI and fractional vegetation cover in the model. Consider a distribution of NDVI versus LAI as in Fig. 5. Given a range of vegetation cover over relatively uniform type of land surface, we extrapolate the curve of NDVI versus LAI through the ordinate of the graph (for which LAI = 0) to obtain the bare soil temperature,  $T_{bs}$ . Leaf temperature is given by the asymptotic temperature  $T_f$ . (The significance of these two temperatures, that of bare soil and leaf, is discussed below.)

In principle, the value of  $T_f$  occurs at infinitely large leaf area index. Sellers' (1985) work, however, shows that the amount of upwelling radiance rapidly approaches saturation above a leaf area index of about 2-3. We suggest that the canopy functions as a homogeneous cover in the asymptotic part of the curve and as a partial cover in the region where LAI changes rapidly with NDVI. We illustrate the relevance of this remark in regard to Fig. 5. Above LAI\* the canopy acts as a complete vegetation cover, a "big leaf" model in which the density of leaves controls the penetration of radiance to or from the ground surface beneath the vegetation cover. Holes exist in the vegetation but they are small and uniformly distributed. Below LAI\* the canopy no longer behaves as a big leaf but as a series of big leaves and bare soil patches with some fractional vegetation cover; the latter may be a function of LAI.

At LAI less than LAI\*, we run two models simultaneously, that for bare soil and that for vegetation with a value of LAI in the vegetation patches equal to some representative value, e.g. LAI\*. The functional relationship between LAI (or NDVI) and fractional vegetation cover is determined empirically as solutions to the boundary layer model for values of LAI less than LAI\*.

We should point out that this technique may not readily apply to low-resolution satellite imagery, because the a wide range of fractional vegetation is unlikely over any small, homogeneous region. Its value, however, is that the use of aircraft data may allow us to derive general functional relationships between LAI (or NFVI) and the fractional vegetation cover and thereby calculate the surface energy fluxes and the substrate moisture content for any value of LAI and surface temperature. Whether the two scales (that of satellite and aircraft) can be meshed remains to be seen from future research.

Given the information in Fig. 5 we can calculate to soil water contents, one appropriate to the temperature of a bare soil surface ( $T_{bs}$ ) and the other for the root zone ( $T_f$ ). Further, it will be interesting to relate the derived fractional vegetation coverage function with the value of LAI for different states of vegetation development. Of course, we may not always obtain a systematic relation between LAI and  $T_s$  as depicted in Fig. 5. Absence of such a relationship simply means that the surface and root zone moisture values do not differ significantly or that the range of LAI over the domain is very small. Scatter may be due also to a dependence of  $T_s$  on other factors such as soil moisture or roughness.

Preliminary results for the 16th of June 1986 suggest that soil moisture values close to zero are necessary in the model in order to yield the high

temperatures of bare soil fields in Fig. 4. In contrast, high soil moistures are required to produce the cool temperatures of the full oats canopy in field N2. Temperatures in field N6 (leaf area index of 1.8) reflect a mixture of bare soil and vegetation.

#### Deviation of leaf area indices from visible radiances

Let us now address the idea of deriving LAI values from visible radiances. Temperature values in Fig. 3 that lie between extremes reflect differing amounts of vegetation. Fig. 6 shows measured and derived leaf area indices as a function of time over field N6 during the HAPEX experiment. Derived leaf area indices were obtained by Taconet (private communication) from two solar channels for AVHRR by computing a normalized difference vegetation index (NDVI) by a regression equation of Bauer et al. (1985). The large discrepancy between derived and measured leaf area indices in June is due to contamination by surrounding bare soil pixels.

### 3. Image analysis

Much of our effort during the past year of the grant has been devoted to completely revising our capabilities at image analysis and model execution. Presently, we have in operation a fast and efficient image processing and modeling work station. Image analysis is performed using the ERDAS system, which has proved to be effective in use by other remote sensing groups; (Fig. 3 was produced by the ERDAS software). The system that drives the ERDAS is an AT&T 6300 computer which is serviced by two 20 megabyte removable disks. This system also executes the model and interfaces it with the image values.

We are analyzing aircraft images of temperature and vegetation index (derived leaf area index) for several days during HAPEX. Infrared temperatures can be determined from the TIMS instrument, which measures

infrared radiances, and the vegetation indices from the NS001 which measured solar radiances. With the kind cooperation of Thomas Schmugge we have received the necessary image data and have begun to analyze all the data for several days during June, 1986. In addition, we have received the AVHRR data from France and we are considering a reworking of Taconet's results given by the LAI(SAT) curve in Fig. 6 in order to see if a better fit with surface measurements can be obtained.

We are examining the water vapor corrections in order to further substantiate the extraordinary high temperatures of the bare soil areas. Eventually, we will examine all the available image data for selected days during HAPEX, derive surface temperatures, leaf area indices and their histograms and test our new ideas and model formulations as discussed above. When the data becomes available, we will investigate the possibility of using the 1987 FIFE images and surface measurements to study the problem of sparse vegetation.

#### 4. Micrometeorological measurements

Virtually every value of every parameter in any boundary layer model, whether one-dimensional or three dimensional, has been derived from point measurements. We regard such measurements as vital in model development. An effort, therefore, has been devoted to obtaining supplementary micrometeorological parameters at an agricultural site, called Rock Springs, which is near Penn State. This measurements program was developed by colleagues to study dry deposition, but has been expanded through our efforts to measure soil moisture, radiometric surface temperature and certain plant parameters: leaf area index and (starting this summer) leaf water potential and leaf stomatal resistance. During the summer we measure surface energy

and momentum fluxes by a variety of systems. Each year the crop changes: wheat in 1986, corn in 1987 and soybeans in 1988.

These measurements are highly relevant to the problem of remote sensing of surface energy fluxes. A fundamental problem in remote sensing is that the latter is capable only of sensing the effects of a bulk canopy resistance to water vapor flux. We instituted radiometer measurements from a mast. These measurements will allow us to calculate surface energy fluxes and the bulk canopy resistance to moisture flux,  $r_c$ . This canopy resistance ( $r_c$ ) differs from stomatal resistance but the two are very closely related in the case of a full vegetation cover (Taconet et al., 1986; Lindroth and Halldin 1986). In Fig. 1,  $r_c$  represents the net resistance of the vegetation canopy and soil to water vapor flux. For large values of LAI  $r_c$  approaches  $r_{st}$ . A current contentious issue in plant micrometeorology is the relationship between  $r_s$ ,  $r_{st}$  and  $r_c$ . We hope that our modeling combined with field measurements will help to resolve this issue.

We are currently developing programs that will allow us to calculate from measurements, parameters directly related to model development and testing. Preliminary results from the 1986 data are shown in Fig. 7. Note that  $r_c$  varies slowly with changing soil water content at high values of the water content; the figure suggests an exponential increase of  $r_c$  as the surface water contents decrease below about 0.18 by volume. (The wilting point of the soil has been determined independently to be about 0.12.) Since the leaf area index was not factored into this graph, we cannot be sure if the curve is partially an artifact due to variation in vegetation cover. Similar curves exist for moisture availability.

## 5. Related Activities

### a) Total daily evapotranspiration

One interesting study carried out as part of our present NASA grant was to investigate a method proposed by Jackson (1977) for obtaining the total daily evapotranspiration from remote measurements of the surface temperature near local noon. Stated briefly, the Jackson "B formulation" is written

$$\overline{R}_n - \overline{LeE}_o = B(T_o - T_a)^n \quad (4)$$

where B and n are constants,  $T_o$  the surface radiometric temperature,  $T_a$  the air temperature,  $\overline{LeE}_o$  the 24 hour evapotranspiration (in  $Wm^{-2}$ ) and  $\overline{R}_n$  the 24 hour integrated net radiation. Our study concerned an analysis of the n and the B values as functions of wind speed, roughness, vegetation cover and altitude of the air temperature measurement. These results are summarized in a paper, to be submitted for publication, by Carlson and Buffum (1988?).

### b) Urban areas

Although we have not been concerned with remote measurements of surface parameters over urban areas for several years, we have had the occasion to return to the periphery of this topic through the interaction with a visiting scientist, Mr. Robert Gillies, who is jointly working on a doctorate in the department of Building Science, the University of Newcastle upon Tyne, where he is currently a staff member. He is also studying for his Master's degree in meteorology from Penn State. Mr. Gillies, who is independently funded, has arrived at Penn State expressly to work with our group and he will be developing our work station capabilities to include analyses of HCMM and NOAA images for various British cities.

## 6. Conclusion

Our efforts have been to (1) resample the visible channel radiances from NS001 data to the infrared temperatures derived from the TIMS data for 4 days during HAPEX. This operation will allow us to prepare diagrams such as Fig. 5, either from our own measurements or using empirical equations from the literature (2) develop the boundary layer coding the model for calculating soil moisture and surface fluxes for partial vegetation cover, (3) test the model using HAPEX data (TIMS; NS001) to evaluate the efficacy of the method and (4) use leaf area index values in conjunction with surface temperatures to derive a fractional vegetation cover as a function of surface temperature in the model, and (5) obtain two-layer (surface; root zone) soil moisture profiles over patchy vegetation.

## Figure Captions

- Fig. 1 Schematic illustration of plant canopy architecture and interface with atmospheric boundary layer above, as employed in current version of 1-dimensional boundary layer model. Fluxes of water vapor ( $L_e E$ ; left and center streams) and sensible heat ( $H$ ; right stream) pass from the ground (subscript  $g$ ) or the leaves (subscript  $l$ ) to the surface layer through air resistances (denoted by letter  $r$  with subscripts  $a$ ,  $b$ ,  $af$  and  $ag$ ) or stomatal resistance ( $r_{st}$ -vapor only). Water vapor passes from the soil to the air through resistance  $r_g$ . Liquid water passes from the root zone to the leaves across the hydraulic potential gap between  $\psi_g$  (ground) and  $\psi_l$  (leaf). Root and stem (xylem) resistances are combined as  $Z_p$ . Substrate water contents are denoted by the symbol  $\theta$  and the soil surface temperature by  $T_g$ . Leaf temperature and vapor pressure are denoted by the symbols  $T_l$  and  $e_l$ , respectively.
- Fig. 2 Schematic representation of the leaf potential function ( $f(\psi_l)$ ) versus the leaf potential ( $\psi_l$ ; solid curve), showing also the increase in the function as the leaf potential falls below that of the ground ( $\psi_g$ ) after sunrise. The leaf transpiration ( $LeE_f$ ) is proportional to the difference between leaf and ground potentials (via equation (2)). The dashed line represents the two-slope linear approximation to the exponential used in our model. The thin dotted line indicates the water limitation threshold potential ( $\psi_c$ ).
- Fig. 3 Thermal image of Lubbon region in France in grey scale (white is warm and black is cold). Numbers are the mean field temperature in degrees C.
- Fig. 4 Vertical distribution of volumetric soil moisture at Lubbon on 16 June 1986, as measured by gypsum blocks in fields N6 (corn) by neutron probe (asterisks) and by gravimetric sampling in field N5 (corn). The vertical bars at the bottom represent averages of 0-5 cm gravimetric water content samples in four fields. The dashed line suggests the mean vertical soil moisture profile.
- Fig. 5 Schematic distribution of radiometric surface temperatures versus leaf area index derived from normalized vegetation index values for individual pixels (dots) and smoothed relationship (dashed line). The bare soil temperature is  $T_{bs}$ , the threshold temperature for patchy vegetation is  $T_*$  (the equivalent of  $LAI_*$ ) and the bulk leaf temperature is  $T_f$ .
- Fig. 6 Leaf area index derived from normalized difference vegetation index (NDVI) measured by AVHRR as a function of date for field N6 ( $LAI(SAT)$ ) and from direct measurement ( $LAI$ ). The vertical arrow below denotes 16 June. Values along  $LAI$  curve refer to height of corn in meters.

## Figure Captions (continued)

- Fig. 7 Bulk canopy resistance to water vapor flux ( $s\ m^{-1}$ ) as a function of volumetric water content at 5 cm depth for wheat during the summer of 1986 at Rock Springs.

## References

- Avissar, R., P. Avissar, Y. Mahrer and B.A. Bravado, 1985: A model to simulate response of plant storvata to environmental conditions. Ag. and Forest Meteor., 34, 21-29.
- Bauer, M.E., K.P. Gallo and C.S.T. Daughtry, 1985: Spectral estimation of absorbed photosynthetically active radiation in corn canopies. Remote Sensing of Environ., 17, 221-232.
- Carlson, T.N., 1986: Regional-scale estimates of surface moisture availability and thermal inertia using remote thermal measurements. Rem. Sens. Rev., 1, 197-247.
- Carlson, T.N. and M.J. Buffum, 1988(?): On estimating the daily evapotranspiration from remotely sensed temperature measurements (to be submitted to J. Clim. and Appl. Meteor.).
- Carlson, T.N., J.K. Dodd, S.G. Benjamin, J.N. Cooper, 1981: Remote estimation of surface energy balance, moisture availability and thermal inertia. J. Appl. Meteor., 20, 67-87.
- Carlson, T.N., F.G. Rose, E.M. Perry, 1984: Regional scale estimates of surface moisture availability from GOES satellite. J. Agron., 76, 972-979.
- Choudbury, B., 1983: Simulating the effects of weather variables and soil water potential on a corn canopy temperature. Ag. Met., 29, 169-182.
- Dwyer, L.M. and D.W. Stewart, 1984: Indicators of water stress in corn. Can. J. Plant. Sci., 64, 537-546.
- Federer, C.A., 1979: A soil-plant atmosphere model for transpiration of availability of soil water. Water Resources Res., 15, 555-562.
- Federer, C.A. and G.W. Gee, 1976: Diffusion resistance and xylem potential in stressed and unstressed northern hardwood trees. Ecology, 57, 975-984.
- Fisher, M.S., D.A. Charles Edwards and M. Ludlow, 19 : An analysis of the effects of repeated short-term soil water deficits on stomatal conductance to carbon dioxide and leaf photosynthesis by the legume macroptilium atropurpureum cv. Siratro. Aust. J. Plant Physiol., 8, 347-357.
- Flores, A.L. and T.N. Carlson, 1987: Etimacion de parametros del suelo combinando un modelo de capa limite con imagenes digitales de GOES. Meteorologica, (Argentina), XV, 77-92.
- Flores, A.L. and T.N. Carlson, 1987: Estimation of surface moisture availability from remote surface temperature measurements. J. Geophys. Res., 92, 9581-9585.

- Jarvis, P.G., 1976: The interpretation of the variations in leaf water potential and stomatal conductance found in canopies in the field. Phil. Trans. R. Soc. London, B, 273, 593-610.
- Korner, C., J.A. Scheel and H. Bauer, 1979: Maximum leaf diffusive conductance in vascular plants. Photosynthesis, 13, 45-82.
- Lindroth, A. and S. Halldin, 1986: Numerical analysis of pine forests evaporation and surface resistancy. Ag. and Forest Meteor., 38, 59-79.
- Perry, E.M. and T.N. Carlson, 1988: A comparison of active microwave soil water content with infrared surface temperatures and surface moisture availability. To be published in Water Resources Research.
- Sellers, P.J., 1985: Canopy reflectance photosynthesis and transpiration. Int. J. Remote Sensing, 6, 1335-1375.
- Stewart, D.W. and L.M. Dwyer, 1983: Stomatal response to plant water deficits. J. Theor. Biol., 104, 655-666.
- Taconet, O., T.N. Carlson, R. Bernard, D. Vidal-Madjar, 1986: Evolution of a surface/vegetation model using satellite infrared surface temperatures. J. Clim. and Appl. Meteor., 25, 1752-1767.
- Thomas, J.C., K.W. Brown and W.B. Jordan, 1976: Stomatal response to leaf water potential affected by preconditioning water stress in the field. Agron. J., 68, 706-708.
- Turner, N.C., 1974: Stomatal behavior and water status of maize, sorghum, and tobacco under field conditions. II. At low-soil water potential. Plant Physiol., 53, 360-365.
- Turner, N.C., 1975: Concurrent comparisons of stomatal behaviors, water status, and evaporation of maize in soil at high or low water potential. Plant Physiol., 55, 932-936.
- Wetzel, P.J. and J.T. Chang, 1987: Concerning the relationship between evapotranspiration and soil moisture. J. Climate and Appl. Meteor., 26, 18-27.
- Wetzel, P.J. and R.H. Woodward, 1987: Soil moisture estimation using GOES-VISRR infrared data: A case study with a simple statistical method. J. Clim. and Appl. Meteor., 26, 107-117.

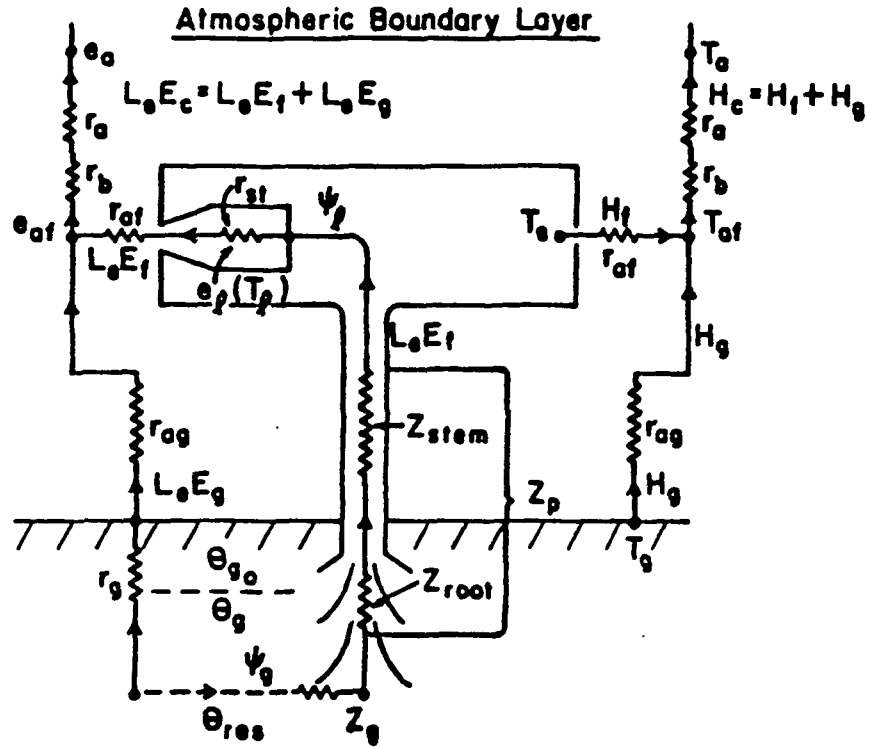


Fig. 1 Schematic illustration of plant canopy architecture and interface with atmospheric boundary layer above, as employed in current version of 1-dimensional boundary layer model. Fluxes of water vapor ( $L_e E$ ; left and center streams) and sensible heat ( $H$ ; right stream) pass from the ground (subscript  $g$ ) or the leaves (subscript  $l$ ) to the surface layer through air resistances (denoted by letter  $r$  with subscripts  $a$ ,  $b$ ,  $af$  and  $ag$ ) or stomatal resistance ( $r_{st}$ -vapor only). Water vapor passes from the soil to the air through resistance  $r_g$ . Liquid water passes from the root zone to the leaves across the hydraulic potential gap between  $\psi_g$  (ground) and  $\psi_l$  (leaf). Root and stem (xylem) resistances are combined as  $Z_p$ . Substrate water contents are denoted by the symbol  $\theta$  and the soil surface temperature by  $T_g$ . Leaf temperature and vapor pressure are denoted by the symbols  $T_l$  and  $e_l$ , respectively.

ORIGINAL PAGE IS  
OF POOR QUALITY

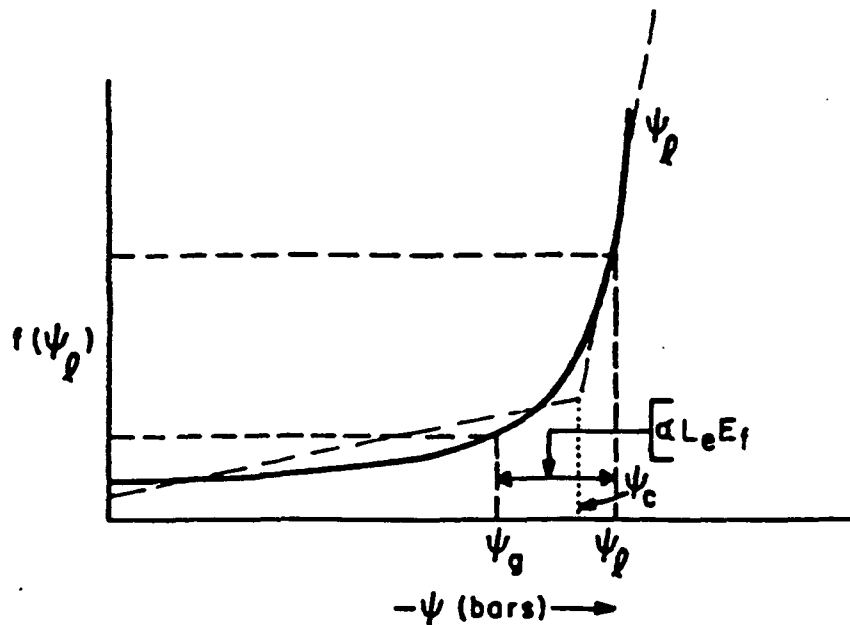


Fig. 2 Schematic representation of the leaf potential function ( $f(\psi_1)$ ) versus the leaf potential ( $\psi_1$ ; solid curve), showing also the increase in the function as the leaf potential falls below that of the ground ( $\psi_g$ ) after sunrise. The leaf transpiration ( $L_e E_f$ ) is proportional to the difference between leaf and ground potentials (via equation (2)). The dashed line represents the two-slope linear approximation to the exponential used in our model. The thin dotted line indicates the water limitation threshold potential ( $\psi_c$ ).

ORIGINAL PAGE IS  
OF POOR QUALITY



Fig. 3 Thermal image of Lubbon region in France in grey scale (white is warm and black is cold). Numbers are the mean field temperature in degrees C.

ORIGINAL PAGE IS  
OF POOR QUALITY

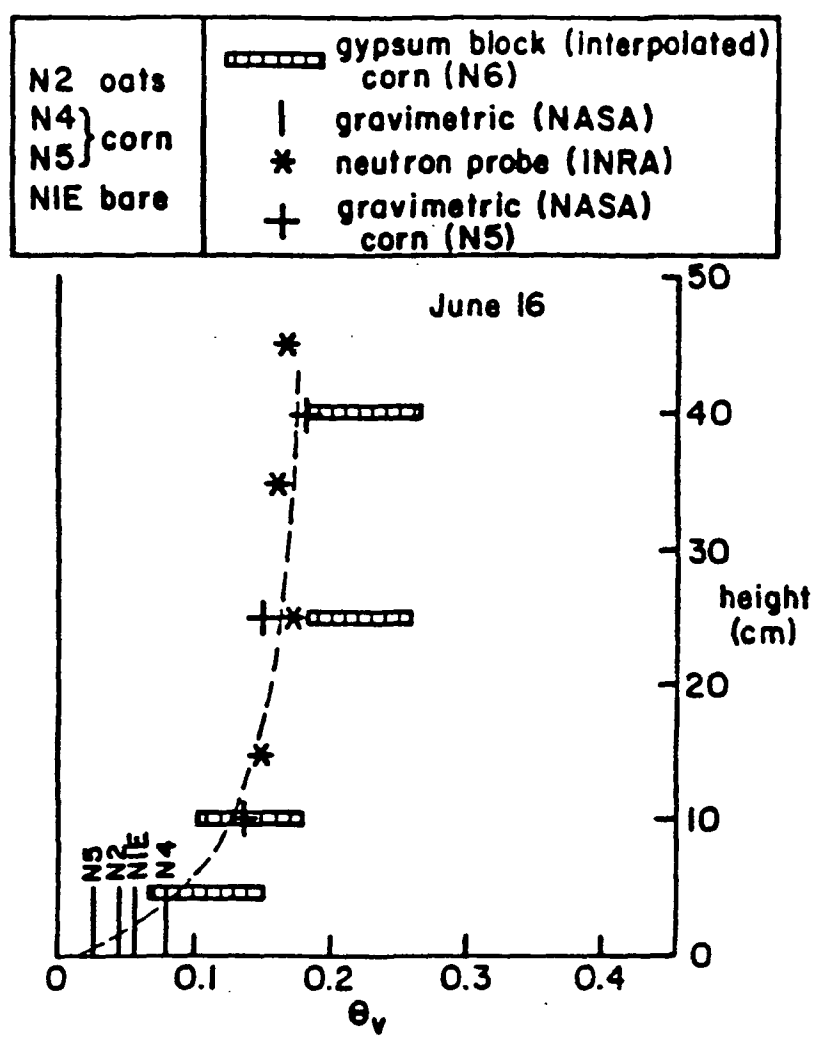


Fig. 4 Vertical distribution of volumetric soil moisture at Lubbon on 16 June 1986, as measured by gypsum blocks in fields N6 (corn) by neutron probe (asterisks) and by gravimetric sampling in field N5 (corn). The vertical bars at the bottom represent averages of 0-5 cm gravimetric water content samples in four fields. The dashed line suggests the mean vertical soil moisture profile.

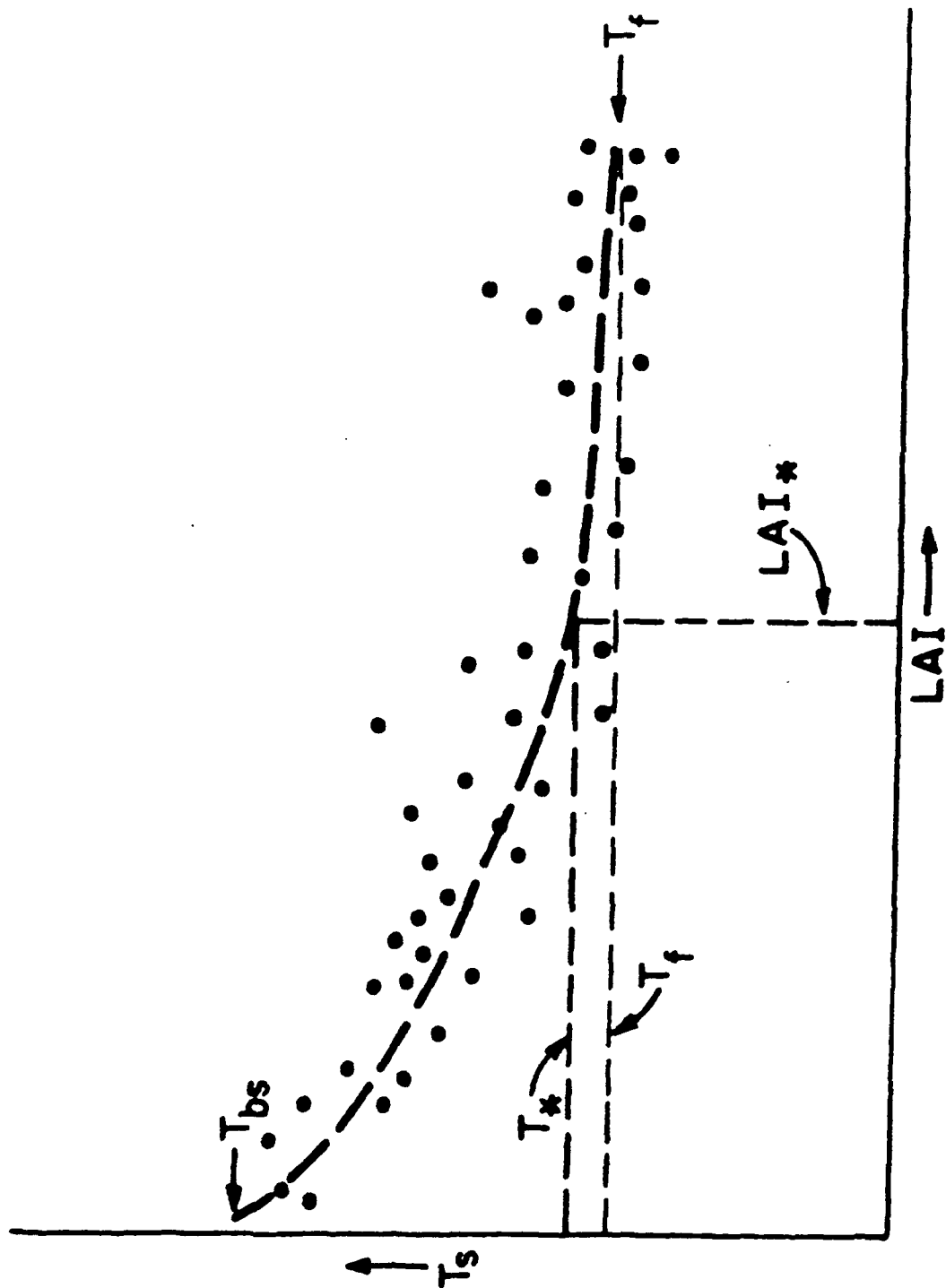


Fig. 5 Schematic distribution of radiometric surface temperatures versus leaf area index derived from normalized vegetation index values for individual pixels (dots) and smoothed relationship (dashed line). The bare soil temperature is  $T_{bs}$ , the threshold temperature for patchy vegetation is  $T^*$  (the equivalent of  $LAI^*$ ) and the bulk leaf temperature is  $T_f$ .

ORIGINAL PAGE IS  
OF POOR QUALITY

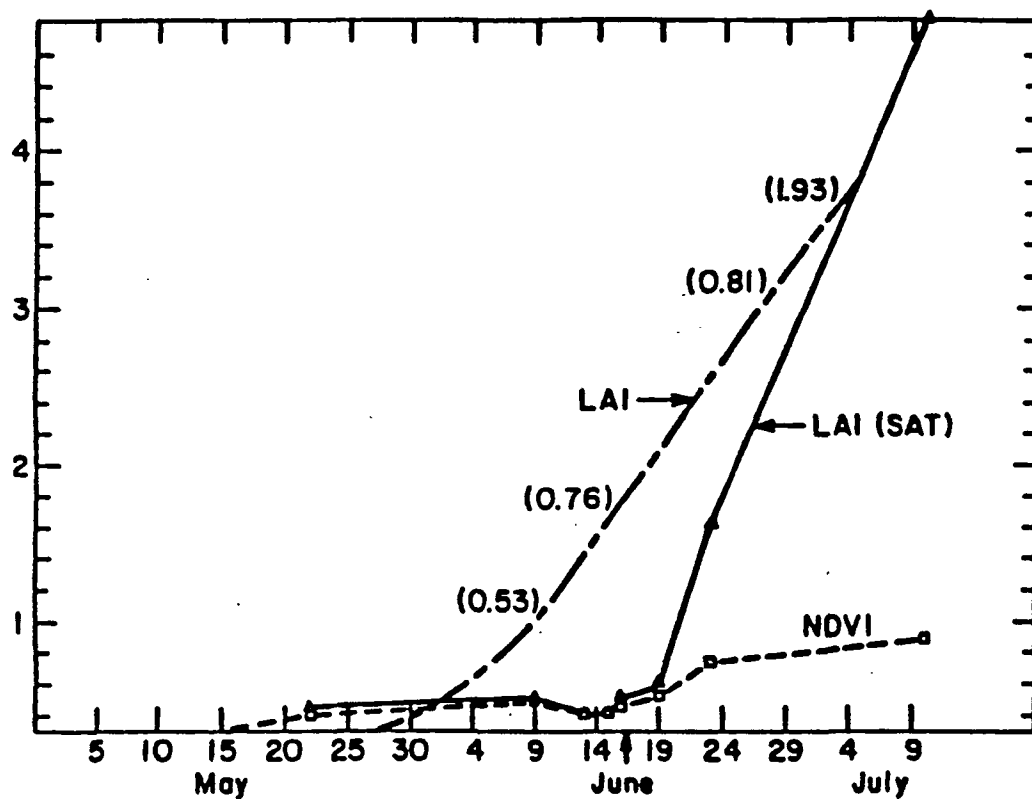


Fig. 6 Leaf area index derived from normalized difference vegetation index (NDVI) measured by AVHRR as a function of date for field N6 (LAI(SAT)) and from direct measurement (LAI). The vertical arrow below denotes 16 June. Values along LAI curve refer to height of corn in meters.

ORIGINAL PAGE IS  
OF POOR QUALITY

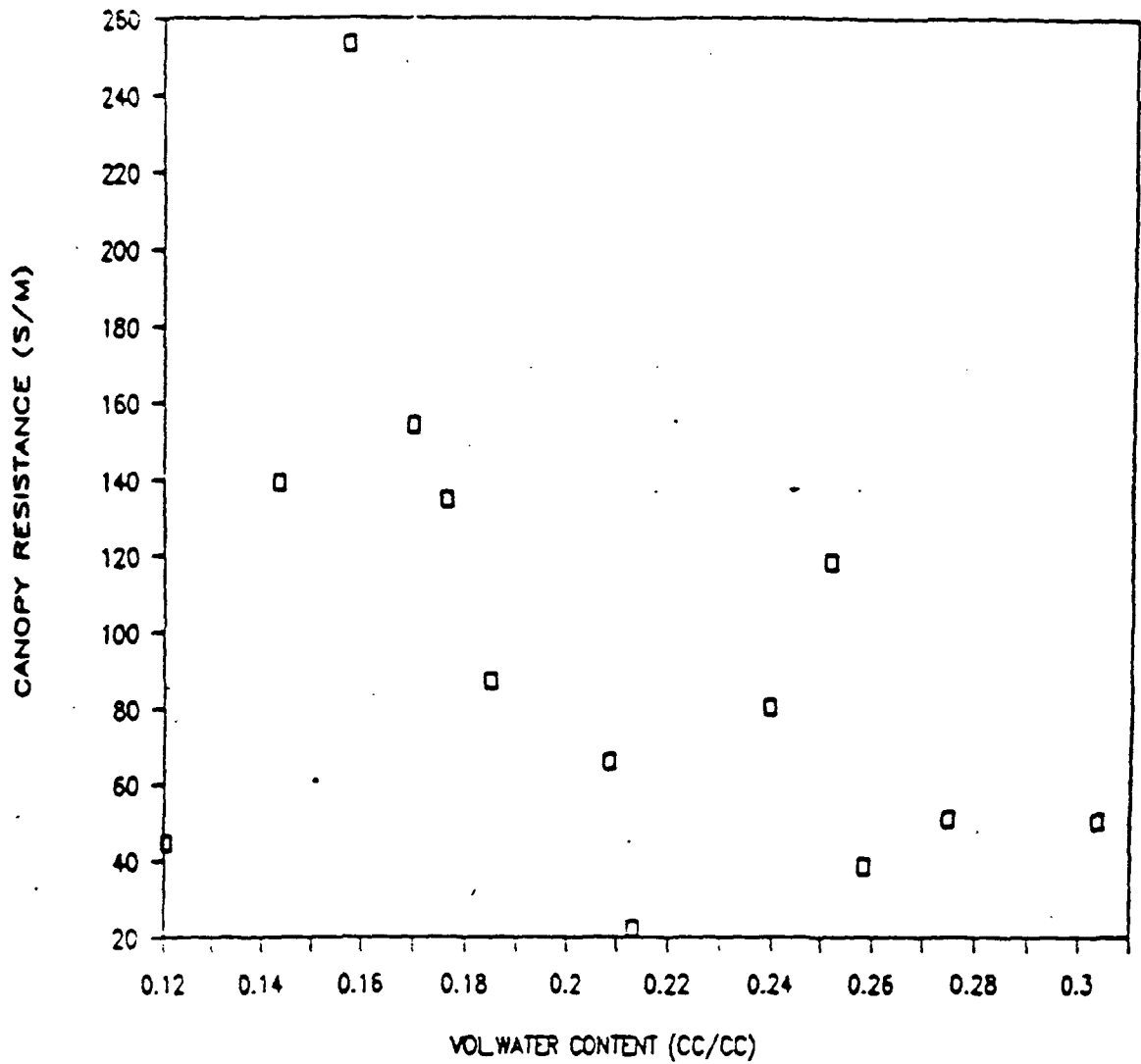


Fig. 7 Bulk canopy resistance to water vapor flux ( $s\ m^{-1}$ ) as a function of volumetric water content at 5 cm depth for wheat during the summer of 1986 at Rock Springs.